Variable Photon Energy Photoelectron Spectroscopic and Theoretical Investigations of the Electronic Structure of $TiCl_4$

Bruce E. Bursten,[†] Jennifer C. Green,*[,‡] Nikolas Kaltsoyannis,[†,‡] Michael A. MacDonald,[§] Kong H. Sze,[‡] and John S. Tse[∥]

Department of Chemistry, The Ohio State University, Columbus, Ohio 43210, Inorganic Chemistry Laboratory, University of Oxford, South Parks Road, Oxford OX1 3QR, U.K., SERC Daresbury Laboratory, Warrington WA4 4AD, U.K., and National Research Council of Canada, Ottawa K1A OR6, Canada

Received February 24, 1994[⊗]

The photoelectron spectrum of $TiCl_4$ has been measured using synchrotron radiation over the incident photon energy range 17−69 eV, and relative partial photoionization cross sections have been derived for the valence bands. Band A ($1t_1^{-1}$) and band B ($3t_2^{-1}$) display cross section variations typical of Cl 3p atomic orbital-localized levels. Bands C+D show cross section enhancement between 40 and 60 eV and are assigned to $1e^{-1}$ and $2t_2^{-1}$. Band E ($2a_1^{-1}$) shows no such feature and has cross section behavior which is appreciably different from that of any of the other bands. The small cross section maximum at 40 eV is attributed to a molecular shape resonance. Discrete variational Xα calculations support this orbital ordering, and quantitative agreement is found between the experimental and calculated ionization energies. Photoionization cross sections were calculated using the multiple-scattering Xα method. Good agreement was found between experimental and theoretical branching ratios, confirming the assignment and suggesting that the resonances found in the $2t_2$ and $2a_1$ orbital cross sections are due to multiple scattering from the localized Cl electrons. The minimum in the $3t_2$ cross section is associated with the Cooper minimum of the Cl 3p orbital.

Introduction

Tetrahedral coordination is one of the geometries central to inorganic chemistry. A thorough knowledge of the electronic structures of tetrahedral molecules is therefore of key importance in understanding a wide range of chemical systems. The structural simplicity, high symmetry, and volatility of $TiCl_4$ have led to extensive experimental investigations via photoelectron spectroscopy (PES),[1−8] and numerous calculational approaches have also been employed.[1,7,9−19] It is perhaps surprising, therefore, that there is still no general agreement as to the assignment of the photoelectron (PE) spectrum of this prototypical molecule. Clearly, this remains a highly desirable goal—an understanding of the bonding in these simple systems is vital in view of the fundamental position which they occupy in coordination chemistry. Furthermore, it is only through an unequivocal assignment of their PE spectra that the success or otherwise of the wide range of theoretical approaches that have been brought to bear can be properly gauged. From the experimental standpoint, it is important that we understand these simple tetrahedral molecules if we are to have confidence in applying our techniques to more complicated transition metal systems.

We recently published a combined theoretical and experimental study of OsO_4,[20] in which ΔSCF and Green's function methods were applied together with synchrotron radiation-based PES to produce a consistent interpretation of the valence PE spectrum. In this paper, we present a similar study of $TiCl_4$, although in this instance local density functional theory (in its discrete variational (DV) form) is the method used for calculation of the ionization energies and ionization cross sections are also calculated using the multiple-scattering (MS) Xα method.[21−24]

Variable photon energy PE spectroscopy (PES) is now established as a powerful tool in electronic structure determination. We and others have investigated a wide range of chemical systems, with examples drawn from both classical coordination[20,25−27] and organometallic chemistry,[20,25−38] and have found the technique to be a sensitive probe of the

[†] The Ohio State University.
[‡] University of Oxford.
[§] SERC Daresbury Laboratory.
[∥] National Research Council of Canada.
[⊗] Abstract published in *Advance ACS Abstracts,* September 15, 1994.

(1) Burroughs, P.; Evans, S.; Hamnett, A.; Orchard, A. F.; Richardson, N. V. *J. Chem. Soc., Faraday Trans. 2* **1974**, *70*, 1895.
(2) Egdell, R. G. Thesis, University of Oxford, 1977.
(3) Egdell, R. G.; Orchard, A. F.; Lloyd, D. R.; Richardson, N. V. *J. Electron Spectrosc. Relat. Phenom.* **1977**, *12*, 415.
(4) Cox, P. A.; Evans, S.; Hamnett, A.; Orchard, A. F. *Chem. Phys. Lett.* **1970**, *7*, 414.
(5) Green, J. C.; Green, M. L. H.; Joachim, P. J.; Orchard, A. F.; Turner, D. W. *Philos. Trans. R. Soc. London, A* **1970**, *268*, 111.
(6) Egdell, R. G.; Orchard, A. F. *J. Chem. Soc., Faraday Trans. 2* **1978**, *74*, 485.
(7) Bancroft, G. M.; Pellach, E.; Tse, J. S. *Inorg. Chem.* **1982**, *21*, 2950.
(8) Wetzel, H. E. Thesis, University of Hamburg, 1987.
(9) Becker, C. A. L.; Dahl, J. P. *Theor. Chim. Acta* **1969**, *14*, 26.
(10) Becker, C. A. L.; Ballhausen, C. J.; Trajberg, I. *Theor. Chim. Acta* **1969**, *13*, 355.
(11) Choplin, F.; Kaufmann, G. *Theor. Chim. Acta* **1972**, *25*, 54.
(12) Truax, D. R.; Geer, J. A.; Ziegler, T. *J. Chem. Phys.* **1973**, *59*, 6662.
(13) Fenske, F. R.; Radtke, D. D. *Inorg. Chem.* **1968**, *7*, 479.
(14) Ellis, D. E.; Parameswan, T. *Int. J. Quantum Chem., Symp.* **1971**, *5*, 443.
(15) Parameswan, T.; Ellis, D. E. *J. Chem. Phys.* **1973**, *58*, 2088.
(16) Tossell, J. A. *Chem. Phys. Lett.* **1979**, *65*, 371.
(17) Foti, A. E.; Smith, V. H.; Whitehead, M. A. *Mol. Phys.* **1982**, *45*, 385.
(18) Hillier, I. H.; Kendrick, J. *Inorg. Chem.* **1976**, *15*, 520.
(19) von Niessen, W. *Inorg. Chem.* **1987**, *26*, 567.
(20) Green, J. C.; Guest, M. F.; Hillier, I. H.; Jarrett-Sprague, S. A.; Kaltsoyannis, N.; MacDonald, M. A.; Sze, K. H. *Inorg. Chem.* **1992**, *31*, 1588.
(21) Johnson, K. H. *Adv. Chem. Phys.* **1973**, *7*, 143.
(22) Dill, D.; Dehmer, J. *J. Chem. Phys.* **1974**, *61*, 692.
(23) Davenport, J. W. *Phys. Rev. Lett.* **1976**, *36*, 945.
(24) *Electron-Molecule and Photon-Molecule Collisions*; Rescigno, T., McKoy, V., Schneider, B., Eds.; Plenum: New York, 1979.

0020-1669/94/1333-5086$04.50/0

localization properties of valence electrons. In particular, the very different partial cross section behavior of d and f electrons with respect to s and p provides extensive information on metal−ligand covalency. The empirical He II/He I intenisty ratio rules[39-48] have been examined more fully, and many of the limitations of the discharge lamp method have been exposed. A variable photon energy investigation of $TiCl_4$ was therefore a logical choice in pursuit of unequivocal spectral assignment, particularly as much of the dispute in the literature is based on experimentally observed He II/He I intensity changes.[7] Further interest stems from the opportunity to compare transition metal with main group compounds, as a detailed investigation of the valence molecular orbital cross sections of CCl_4[49] and $SiCl_4$[50] has already been done. It was hoped that halogen- and central atom-derived effects would be distinguished more easily through this comparison.

Experimental Section

The PE spectra of $TiCl_4$ were obtained using the synchrotron radiation source at the Science and Engineering Research Council Daresbury Laboratory. A full account of our experimental method has been given,[28] and the apparatus and its performance are described elsewhere.[51] Hence only a brief account of experimental procedures is given here.

Synchrotron radiation from the 2 GeV electron storage ring at the SERC Daresbury Laboratory was monochromated using a toroidal grating monochromator and was used to photoionize gaseous samples in a cylindrical ionization chamber. The photoelectrons were energy-analyzed using a three-element zoom lens in conjunction with a hemispherical electron energy analyzer, which was positioned at the "magic angle" so as to eliminate the effects of the PE asymmetry parameter, β, on signal intensity. Multiple-scan PE spectra were collected at each photon energy required. The decay of the storage ring beam current was corrected for by linking the scan rate with the output from a photodiode positioned to intersect the photon beam after it had passed through the ionization region. The sensitivity of the photodiode to different radiation energies was determined by measuring the np^{-1} PE spectra of Ne, Ar, and Xe. This procedure ensures that the band intensity of the final spectrum divided by the number of scans gives a measure of the cross section at any particular photon energy. The rare gas data were also used to characterize and correct for a falloff in analyzer collection efficiency at PE kinetic energies <15 eV. Photoionization cross sections for the rare gases were taken from the literature.[52,53]

Sample pressure fluctuations were corrected for by collecting a "standard" calibration spectrum before and after each data spectrum. The integrated intensities of the bands in these spectra were then used as a relative measure of the sample density in the ionization region.

$TiCl_4$ is sufficiently volatile that it could be held outside the spectrometer and allowed to sublime into the chamber through a needle valve. A liquid nitrogen-cooled finger was fitted to the spectrometer to prevent diffusion of compound into the pumps.

Band areas were obtained by deconvoluting the spectra using asymmetric Gaussian functions. Relative partial photoionization cross sections (RPPICSs) were derived from these band areas using a suite of programs initially developed by Glyn Cooper and J.C.G. and subsequently installed on the Convex C220 supercomputer at the Daresbury Laboratory. The cross sections are relative, as we have no measure of the absolute pressure in the photoionization region; they are partial, as measurements have only been made at the magic angle.

$TiCl_4$ was obtained from Fluorochem Ltd. and purified in vacuo.

Computational Methodology and Details

Density functional methods are gaining increasing acceptance as powerful tools for the calculation of the electronic structure and properties of molecules,[54] and the discrete variational (DV) Xα approach of Ellis[55] is one of its most well-known implementations. Density functional theories lead to a one-electron eigenvalue equation incorporating a Coulomb operator, which accounts for the nuclear attraction and electron−electron repulsion, and a local exchange-correlation operator. The simplest choice for this operator is Slater's Xα potential,[56,57] although the improved parametrization of Hedin and Lundqvist[58] has been employed in the calculations reported herein.

The molecular orbitals (MOs) are expressed as a linear combination of atomic orbitals expansion in a basis of numerical atomic functions obtained from Hartree−Fock−Slater calculations on neutral atoms and cations and subsequently combined to provide a "multi-ζ" basis of approximately split-valence quality.[59] The self-consistent-multipolar charge density representation is used in evaluating the molecular Coulomb integrals.[60] A Mulliken population analysis[61] is employed in order to provide an approximate estimation of the molecular charge density.

(25) Green, J. C.; Kaltsoyannis, N.; MacDonald, M. A.; Sze, K. H. *Chem. Phys. Lett.* **1990**, *175*, 359.
(26) Green, J. C.; Kaltsoyannis, N.; MacDonald, M. A.; Sze, K. H. *J. Chem. Soc., Dalton. Trans.* **1991**, 2371.
(27) Brennan, J. B.; Green, J. C.; Redfern, C. M.; MacDonald, M. A. *J. Chem. Soc., Dalton Trans.* **1990**, 1907.
(28) Cooper, G.; Green, J. C.; Payne, M. P.; Dobson, B. R.; Hillier, I. H. *J. Am. Chem. Soc.* **1987**, *109*, 3836.
(29) Cooper, G.; Green, J. C.; Payne, M. P. *Mol. Phys.* **1988**, *63*, 1031.
(30) Brennan, J. B.; Green, J. C.; Redfern, C. M. *J. Am. Chem. Soc.* **1989**, *111*, 2373.
(31) Brennan, J. G.; Cooper, G.; Green, J. C.; Kaltsoyannis, N.; MacDonald, M. A.; Payne, M. P.; Redfern, C. M.; Sze, K. H. *Chem. Phys.* **1992**, *164*, 276.
(32) Davies, C. E.; Green, J. C.; Kaltsoyannis, N.; MacDonald, M. A.; Qin, J.; Rauchfuss, T. B.; Redfern, C. M.; Stringer, G. H.; Woolhouse, M. G. *Inorg. Chem.* **1992**, *31*, 3779.
(33) Didziulis, S. V.; Cohen, S. L.; Gewirth, A. A.; Solomon, E. I. *J. Am. Chem. Soc.* **1988**, *110*, 250.
(34) Butcher, K. D.; Didziulis, S. V.; Briat, B.; Solomon, E. I. *J. Am. Chem. Soc.* **1990**, *112*, 2231.
(35) Butcher, K. D.; Gebhard, M. S.; Solomon, E. I. *Inorg. Chem.* **1990**, *29*, 2067.
(36) Yang, D. S.; Bancroft, G. M.; Puddephatt, R. J.; Tan, K. H.; N., C. J.; Bozek, J. D. *Inorg. Chem.* **1990**, *29*, 4956.
(37) Li, X. R.; Bancroft, G. M.; Puddephatt, R. J.; Hu, Y. F.; Liu, Z.; Tan, K. H. *Inorg. Chem.* **1992**, *31*, 5162.
(38) Li, X. R.; Bancroft, G. M.; Puddephatt, R. J.; Hu, Y. F.; Liu, Z.; Sutherland, D. G. J.; Tan, K. H. *J. Chem. Soc. Chem. Commun.* **1993**, 67.
(39) Eland, J. H. D. *Photoelectron Spectroscopy*; Butterworths: London, 1984.
(40) Turner, D. W.; Baker, C.; Baker, A. D.; Brundle, C. R. *Molecular Photoelectron Spectroscopy*; Wiley-Interscience: London, 1970.
(41) Rabalais, J. W. *Principles of Ultraviolet Photoelectron Spectroscopy*; Wiley-Interscience: New York, 1977.
(42) Carlson, T. A. *Photoelectron and Auger Spectroscopy*; Plenum: New York, 1975.
(43) Briggs, D. *Handbook of X-ray and ultra-violet photoelectron spectroscopy*; Heyden: London, 1977.
(44) Brundle, C. R., Baker, A. D., Eds. *Electron Spectroscopy. Theory, Techniques and Applications*; Academic Press: London, 1977−1981; Vols. 1−5.
(45) Ghosh, P. K. *Introduction to Photoelectron Spectroscopy*; Wiley-Interscience: New York, 1983.
(46) Furlani, C.; Cauletti, C. *Struct. Bonding* **1977**, *35*, 119.
(47) Cowley, A. H. *Prog. Inorg. Chem.* **1979**, *26*, 46.
(48) Green, J. C. *Struct. Bonding* **1981**, *43*, 37.
(49) Carlson, T. A.; Krause, M. O.; Grimm, F. A.; Keller, P.; Taylor, J. W. *J. Chem. Phys.* **1982**, *77*, 5340.
(50) Carlson, T. A.; Fahlman, A.; Krause, M. O.; Whitley, T. A.; Grimm, F. A.; Piancastelli, M. N.; Taylor, J. W. *J. Chem. Phys.* **1986**, *84*, 641.
(51) Potts, A. W.; Novak, I.; Quinn, G. V.; Dobson, B. R.; Hillier, I. H. *J. Phys. B* **1985**, *18*, 3177.
(52) West, J. B.; Marr, G. V. *Proc. R. Soc. London, A* **1976**, *349*, 397.
(53) West, J. B.; Morton, J. *At. Data Nucl. Data Tables* **1978**, *22*, 103.
(54) Schneider, W. F.; Strittmatter, R. J.; Bursten, B. E.; Ellis, D. E. *Density Functional Methods in Chemistry*; Springer-Verlag: New York, 1991; Chapter 16.
(55) Ellis, D. E. *J. Phys. B: At. Mol. Phys.* **1977**, *10*, 1.
(56) Slater, J. C. *Adv. Quantum Chem.* **1972**, *6*, 1.
(57) Slater, J. S. *Phys. Rev.* **1951**, *81*, 385.
(58) Hedin, L.; Lundqvist, B. I. *J. Phys. C: Solid State Phys.* **1971**, *4*, 2064.
(59) Schneider, W. F. Ph.D. Thesis, The Ohio State University, 1991.

The familiar transition state method of Slater[56,62] is used to calculate the ionization energies. Ground state MO energy differences are often misleading, particularly when the localization properties of the orbitals between which the electron is moved are significantly different.

A metal−ligand distance of 2.185 Å was used for tetrahedral $TiCl_4$.[19]

The DV calculations were performed on the Cray Y-MP supercomputer at the Ohio Supercomputing Centre.

The photoionization cross sections for the valence orbitals of $TiCl_4$ were calculated as a function of the photon energy using the multiple-scattering (MS) Xa method. The accuracy of this method has been demonstrated for many molecules, and in most cases the theoretical results have been shown to be very reliable. The theoretical foundation for this method has been documented elsewhere[21−24] and will not be repeated here. The relevant parameters for the calculations were chosen as follows. The atomic parameters for the exchange-correlation potential compiled by Schwarz[63] were used for the atomic regions. A weighted-average exchange parameter according to the number of the valence electrons of the Ti and Cl atoms was used in the intersphere and outer-sphere regions. To avoid arbitrariness in the choice of sphere sizes, the nonempirical procedure suggested by Norman was followed.[64] The resulting sphere radii are 6.7212, 2.4578, and 2.5921 Å for the outer, Ti, and Cl spheres, respectively. A Latter tail correction was added to the exchange-correlation potential in both ground and continuum states calculations to ensure the correct asymptotic behavior.[65] In the ground state calculation, the expansions of the spherical waves were truncated at $l_{max} = 5$, 3, and 3 for the outer, Ti, and Cl spheres, respectively. Since the continuum wave functions are mainly located in the outer-sphere region, the convergence of the calculated photoionization cross section is very sensitive to the completeness of the angular momentum expansion.[66] This is particularly important for continuum wave functions at high energies. To this end, cross section calculations were performed with $l_{out} = 7-10$ and $l_{atom} = 4$. No significant changes in the calculated photoionization cross sections were observed among these calculations, indicating the l expansion has largely converged.

Results and Discussion

In order to understand the PE spectrum of $TiCl_4$, it is necessary to establish a bonding model for the interaction of a transition metal with a tetrahedral Cl_4 ligand field. We do this in two parts, first through a qualitative approach and subsequently via the results of a DV−Xα calculation. We also calculate the ionization energies (IEs) of the valence MOs and and their photoionization cross sections and use this evidence in conjunction with experimental cross section data to assign the PE spectrum.

Synchrotron radiation has been used previously to investigate the PE spectrum of $TiCl_4$. Wetzel reports the results of a similar study in his Ph.D. thesis,[8] which provides a valuable comparison with our work and that on the closely related CCl_4 and $SiCl_4$.

(i) Bonding and Interpretation of the PE Spectrum. The valence electronic structures of the d^0 MCl_4 species are of the form

$$1a_1^2 1t_2^6 2a_1^2 1e^4 2t_2^6 3t_2^6 1t_1^6$$

where the numbering scheme ignores orbitals correlating with the core orbitals of the constituent atoms. A schematic MO diagram showing the possible atomic contributions to the various MOs is given in Figure 1. The $1a_1$ and $1t_2$ are essentially Cl 3s orbitals. Of the remaining occupied levels, the $2a_1$ and $2t_2$ are traditionally associated with M−Cl σ bonding and the 1e and $3t_2$, with M−Cl π bonding, although there is no σ/π separability of the t_2 orbitals in T_d symmetry. In the absence of any f-orbital contribution from the central atom, the $1t_1$ MO is nonbonding.

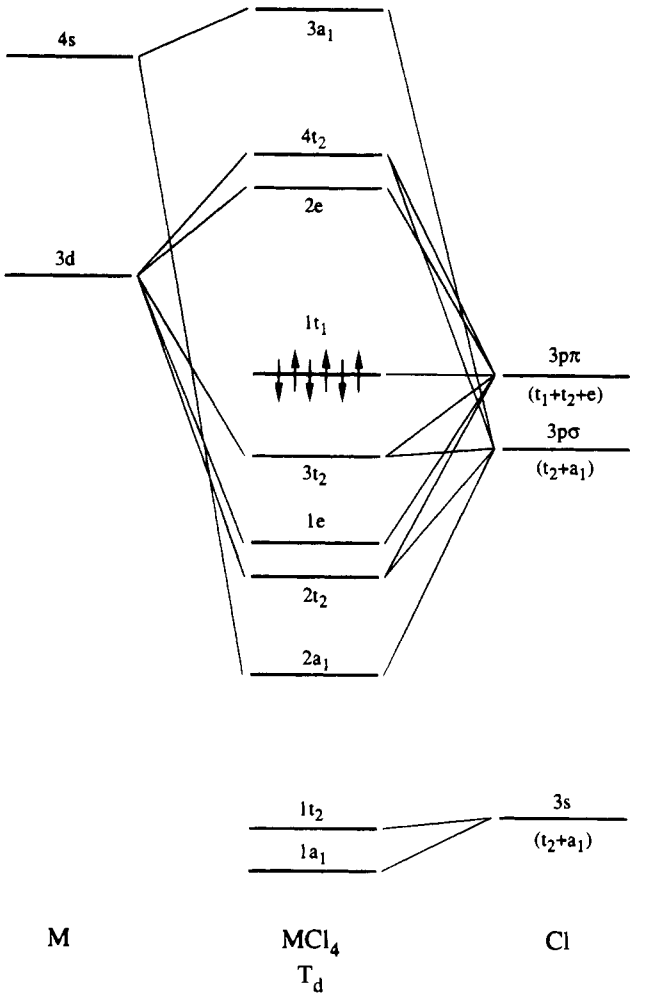

Figure 1. Qualitative molecular orbital diagram for a first-row transition metal in a tetrahedral Cl_4 ligand field.

Table 1. Molecular Orbital Energies and Percent Compositions (Mulliken Population Analysis) of the Valence Levels of $TiCl_4$, Calculated via the Nonrelativistic DV−Xα Approach

mol orbital	energy (eV)	% Ti	% Cl	ionizn energy (eV)[a]
$4t_2$	−4.947	70.49 (3d)	29.41	
2e	−5.716	76.59 (3d)	23.41	
$1t_1$ (HOMO)	−9.060	0.00	100.00	−11.846
$3t_2$	−10.025	7.43 (3d)	92.57	−12.761
1e	−10.420	28.96 (3d)	71.04	−13.233
$2t_2$	−10.704	22.01 (3d)	77.99	−13.561
$2a_1$	−11.106	5.60 (4s)	94.40	−13.921

[a] Calculated via the transition state method.

Table 1 presents the results of our DV−Xα calculation on $TiCl_4$. In performing this calculation, we followed a long line of previous investigations, ranging from approximate techniques such as CNDO,[9−11] through density functional approaches,[14−16] to ab initio[18] and Green's function[19] calculations. An excellentsummary of the theoretical investigations is provided by von

(60) Delley, B.; Ellis, D. E. *J. Chem. Phys.* **1982**, *76*, 1949.
(61) Mulliken, R. S. *J. Chem. Phys.* **1955**, *23*, 1833, 1841, 2338, 2343.
(62) Slater, J. S. *The calculation of molecular orbitals*; Wiley: New York, 1979.
(63) Schwarz, K. *Phys. Rev. B* **1972**, *5*, 2466.
(64) Norman, J. G. *Mol. Phys.* **1976**, *31*, 1191.
(65) Latter, L. *Phys. Rev.* **1955**, *99*, 510.
(66) Wallace, S. R. Ph.D. Dissertation Thesis, Boston University, 1980.

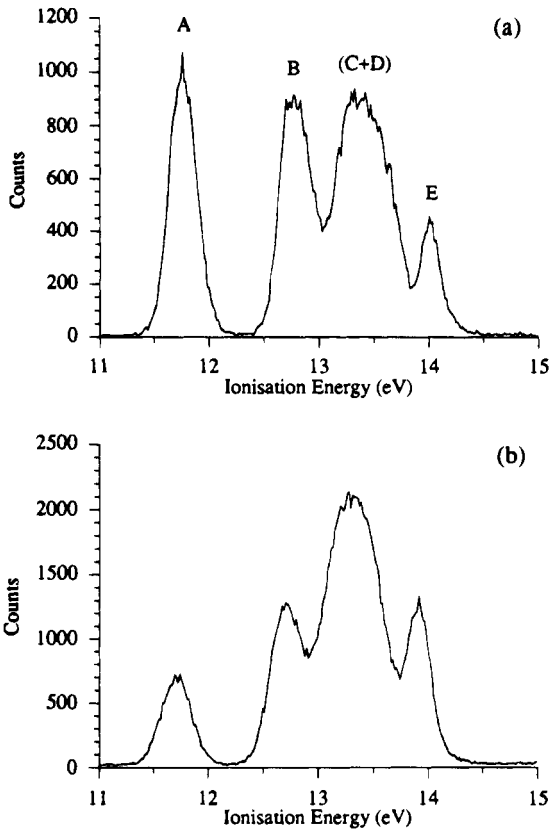

Figure 2. Photoelectron spectra of $TiCl_4$, acquired with synchrotron radiation at (a) 24 and (b) 40 eV.

Table 2. IEs and Band Assignments for the PE Spectrum of $TiCl_4$

band	IE (eV)[a]	refs 1–6, 8, 14–16, 19, 20, 23, 24	refs 7, 17, 18, 21, 22
A	11.69	$^2T_1$	$^2T_1$
B	12.67	$^2T_2$	$^2T_2$
(C+D)	13.17, 13.46	$^2T_2$, ^2E	^2E, $^2A_1$
E	13.91	$^2A_1$	$^2T_2$

[a] Data from ref 7.

to ab initio[18] and Green's function[19] calculations. An excellent summary of the theoretical investigations is provided by von Niessen,[19] and we do not give a detailed comparison of the different methods here. We include our DV–Xα results to provide a starting point for discussion of the localization of the valence MOs and to illustrate how well they reproduce the experimentally determined ionization spectrum (vide supra). The MS–Xα method gave a similar orbital ordering except that the positions of $2t_2$ and $2a_1$ were reversed.

All five MOs $2a_1$–$1t_1$ have predominant Cl 3p AO character, the $1t_1$ rigorously so by symmetry. A small Ti 4s contribution is calculated for the $2a_1$ MO, with metal d admixture in the $2t_2$, 1e, and $3t_2$ orbitals. Of these, the most significant d-orbital content lies in the $2t_2$ and 1e, while the $3t_2$ are found to be well over 90% Cl 3p in character. Including Ti 4p orbitals made no significant difference in the results.

In the valence PE spectrum of $TiCl_4$, therefore, five primary ion states are expected, corresponding to ionization of the $2a_1$–$1t_1$ MOs. Figure 2 presents the spectrum of $TiCl_4$, obtained with synchrotron radiation at 24 and 40 eV, and displays four bands, labeled A, B, (C+D), and E for consistency with previous works. The figures represent the summed spectra rather than an individual scan; consequently, the counts given in Figure 2 do not give a measure of the relative cross sections at the two photon energies. IEs and band assignments are collected in Table 2. From a comparison of Tables 1 and 2 it can be seen that the DV–Xα method in conjunction with the transition state formalism provides virtually quantitative agreement with experiment, the *greatest* discrepancy in the calculated IEs being 0.16 eV. Table 2 indicates that there are essentially two different assignments proposed for the valence bands, the discussion centering chiefly on the order of the $2a_1$ and $2t_2$ MOs. The only PES experiment to favor the assignment of band E to the $2t_2$ is that of Bancroft et al.,[7] in which He II/He I intensity changes are cited as a central piece of evidence, providing further impetus for a synchrotron radiation-based study and cross section calculations.

Table 3. RPPICSs of Bands A–E in the PE Spectrum of $TiCl_4$[a]

$h\nu$ (eV)	band A	band B	band (C+D)	band E
17.00	594(4) × 10^2	544(4) × 10^2	1496(9) × 10^2	169(2) × 10^2
18.00	487(3) × 10^2	509(4) × 10^2	1207(8) × 10^2	148(2) × 10^2
19.00	456(2) × 10^2	492(4) × 10^2	1037(8) × 10^2	125(2) × 10^2
20.00	394(3) × 10^2	482(4) × 10^2	935(8) × 10^2	146(2) × 10^2
21.00	392(3) × 10^2	468(4) × 10^2	811(7) × 10^2	133(2) × 10^2
24.00	285(2) × 10^2	302(2) × 10^2	548(4) × 10^2	109(1) × 10^2
25.00	272(2) × 10^2	283(2) × 10^2	491(4) × 10^2	116(1) × 10^2
26.00	210(1) × 10^2	231(1) × 10^2	390(3) × 10^2	102(1) × 10^2
27.00	204(1) × 10^2	216(2) × 10^2	367(3) × 10^2	102(1) × 10^2
28.00	182(1) × 10^2	194(1) × 10^2	331(3) × 10^2	91(1) × 10^2
30.00	122(1) × 10^2	126(1) × 10^2	225(2) × 10^2	582(7) × 10
32.00	758(6) × 10	763(6) × 10	142(1) × 10^2	350(4) × 10
34.00	481(5) × 10	443(4) × 10	901(9) × 10	218(3) × 10
36.00	332(3) × 10	306(3) × 10	595(6) × 10	174(3) × 10
38.00	217(3) × 10	223(3) × 10	442(5) × 10	156(2) × 10
40.00	196(2) × 10	385(2) × 10	103(1) × 10^2	314(2) × 10
41.50	187(4) × 10	301(5) × 10	125(1) × 10^2	311(5) × 10
43.00	181(4) × 10	271(5) × 10	157(2) × 10^2	215(4) × 10
46.00	177(4) × 10	321(6) × 10	167(2) × 10^2	193(4) × 10
49.00	205(5) × 10	365(6) × 10	179(2) × 10^2	189(5) × 10
52.00	301(5) × 10	399(6) × 10	166(2) × 10^2	204(4) × 10
55.00	337(5) × 10	396(5) × 10	139(1) × 10^2	167(3) × 10
58.00	326(4) × 10	408(5) × 10	106(1) × 10^2	137(3) × 10
62.00	327(4) × 10	366(4) × 10	837(8) × 10	107(2) × 10
64.00	350(4) × 10	375(4) × 10	766(8) × 10	102(2) × 10
66.00	321(3) × 10	322(3) × 10	750(7) × 10	88(2) × 10
69.00	234(2) × 10	249(2) × 10	677(6) × 10	66(1) × 10

[a] Errors are statistical,[76] associated with band area measurements.

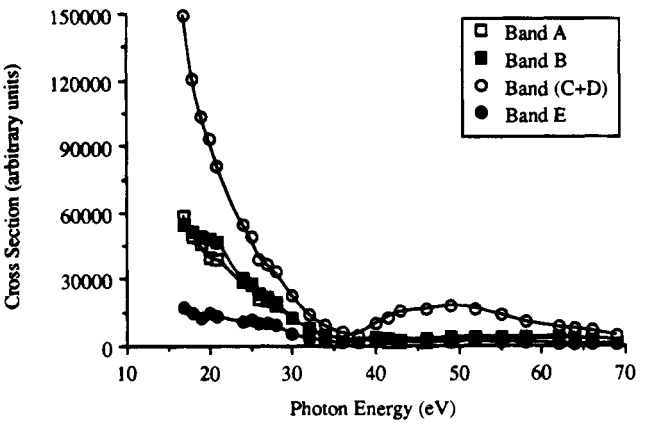

Figure 3. Relative partial photoionization cross sections of bands A–E in the photoelectron spectrum of $TiCl_4$.

(ii) Relative Partial Photoionization Cross Section Results. The valence PE spectrum of $TiCl_4$ has been measured over the incident photon energy range 17–69 eV, and relative partial photoionization cross sections (RPPICSs) have been determined for the four bands A, B, (C+D), and E. The cross section data are given in Table 3 and presented graphically in Figures 3 (all bands) and 4 (individual plots).

The cross section of band A shows a rapid falloff at low incident photon energies, with a shallow minimum at 46 eV

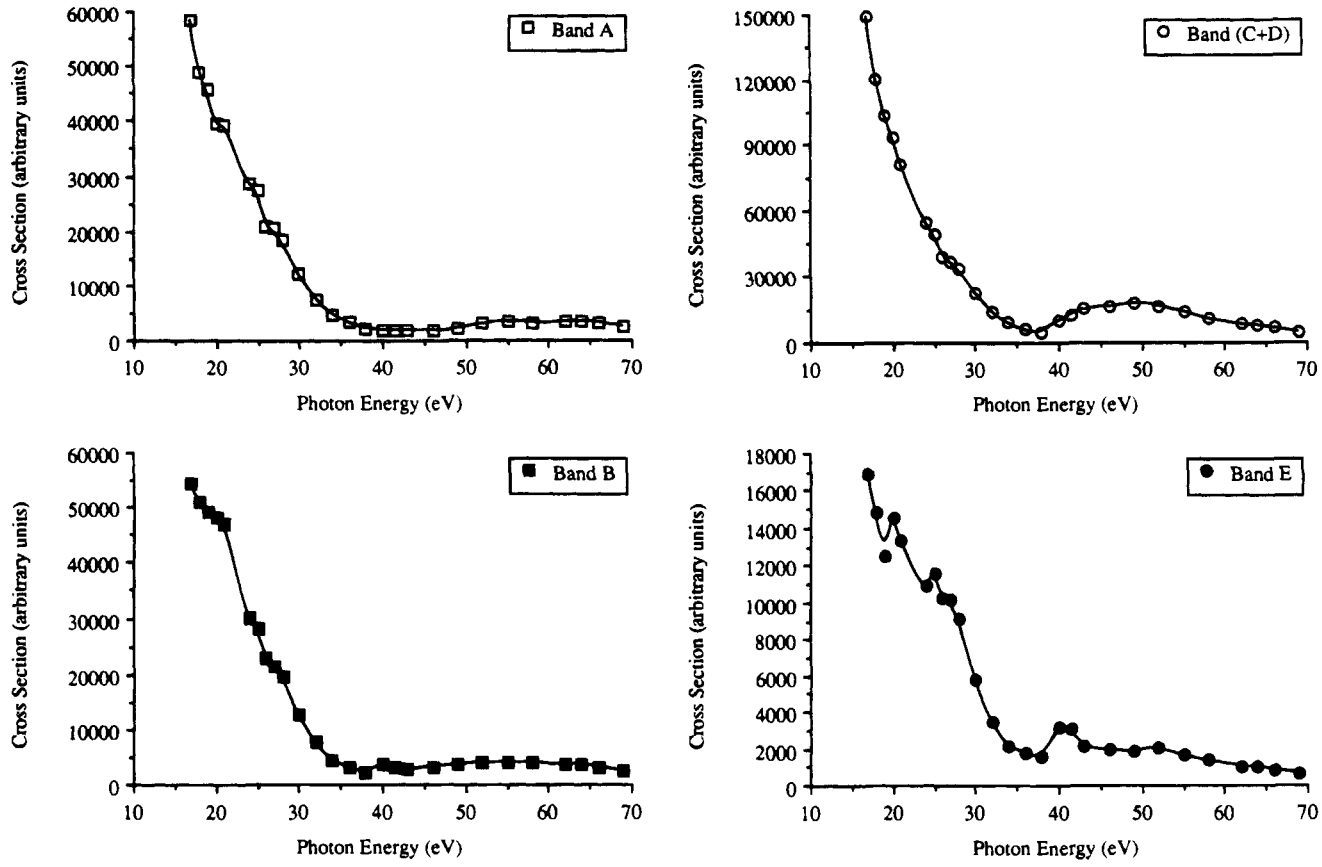

Figure 4. Individual relative partial photoionization cross sections of bands A, B, (C+D), and E in the photoelectron spectrum of $TiCl_4$.

and a subsequent small maximum at 64 eV. The generally accepted assignment of this band to the $1t_1$ MO indicates that the only AO contributions to this MO come from the Cl atoms, as none of the valence AOs of Ti transform as t_1 in T_d symmetry. Thus the cross section behavior of this band should be very similar to that of the equivalent bands in the PE spectra of CCl_4 and $SiCl_4$, i.e. independent of the central atom.

The rapid falloff at low photon energies is typical of the cross section behavior of s and p AOs of and MOs composed largely of such functions. It arises because the interaction of the outgoing electron wave function with the ground electronic state decreases owing to the oscillatory nature of the former. The ionization dipole matrix elements begin to cancel,[67] and the cross section decreases. There are a number of effects which modify this monotonic cross section falloff, and although these are principally associated with higher angular momentum electrons, one that is also found in ligand-based ionizations is the Cooper minimum.

Cooper minima are a well-established effect in both atomic and molecular photoionization cross sections[68,69] and arise because the photoionization dipole matrix element for a given transition goes through zero due to the exact cancellation of positive and negative contributions. The minima are not usually zero minima because while the $3p \rightarrow \epsilon d$ transition dipole matrix element for a given element (e.g. Cl) may go through zero at a given incident photon energy, that for the $3p \rightarrow \epsilon s$ will not. An important feature of Cooper minima is that they occur only in subshells whose wave functions possess radial nodes.

In their work on CCl_4 and $SiCl_4$, Carlson et al. discuss the Cooper minimum in molecules.[49,50] The cross section behavior of the $1t_1^{-1}$ bands in both main group molecules is very similar to that of band A in $TiCl_4$, with a shallow minimum at 43 eV (CCl_4) and 42 eV ($SiCl_4$) incident photon energy. This minimum is assigned to the Cooper minimum of the 3p AO of Cl, which has subsequently been calculated to occur at a PE kinetic energy of ca. 30 eV.[70] This theoretical result compares favorably with the experimental values of 31.4 eV for CCl_4, 30.0 eV for $SiCl_4$, and 34.2 eV for $TiCl_4$. There is therefore little doubt that the RPPICS of band A can be adequately explained in terms of an MO strongly localized on the Cl atoms. As the cross section variations of band A are very similar to those found for the $1t_1^{-1}$ band in the previous synchrotron study of $TiCl_4$,[8] all of the variable photon energy studies are in agreement as to the assignment and cross section behavior of the first ionization band of these tetrachlorides.

We calculate the $3t_2$ MO to be over 90% Cl 3p in character (Table 1), a result supported by previous ab initio calculations.[18] Band B is therefore expected to show RPPICS behavior similar to that of band A. This is indeed found to be the case, with two minor differences. There is a slight shoulder to the RPPICS falloff at 21 eV photon energy and a small maximum at 40 eV, neither of which is seen in the cross sections of the equivalent bands of CCl_4 and $SiCl_4$. The data for the $3t_2^{-1}$ band from the previous synchrotron study of $TiCl_4$ do not begin at a sufficiently low incident photon energy to distinguish the cross section shoulder but does find a small maximum at 40 eV.

The assignment of bands A and B has not been the subject of debate, unlike that of bands (C+D) and E. Either band (C+D) contains the 1e and $2t_2$ MOs, with the $2a_1$ assigned to band E, or the $2t_2$ and $2a_1$ MO ordering is reversed. The analysis of the RPPICSs of these two bands attempts to resolve this dilemma.

(67) Heitler, W. *Quantum Theory of Radiation*; Oxford University Press: London, 1954.
(68) Cooper, J. W. *Phys. Rev.* **1962**, *128*, 681.
(69) Cooper, J. W. *Phys. Rev. Lett.* **1964**, *13*, 762.
(70) Yeh, J. J.; Lindau, I. *At. Data Nucl. Data Tables* **1985**, *32*, 1.

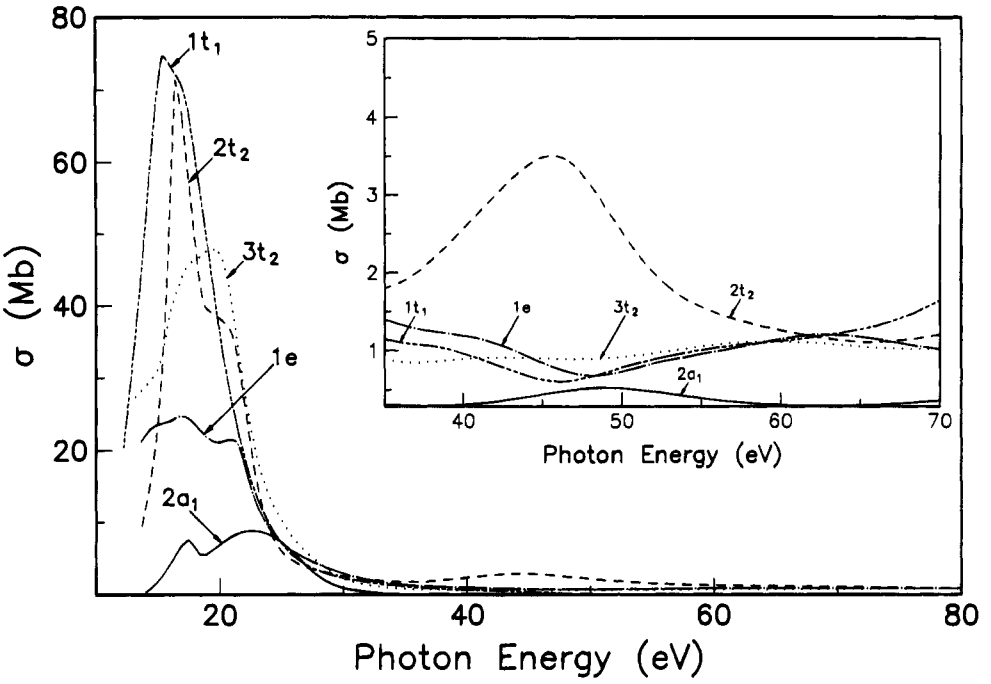

Figure 5. Theoretical photoionization cross sections for the valence orbitals of $TiCl_4$.

The cross section behavior of band (C+D) is different from those of bands A and B in having a much more pronounced maximum following the initial falloff (Figures 3 and 4). The MOs ionizing under band (C+D), whatever their assignment, will be predominantly Cl 3p in character, and it is therefore difficult to explain the much larger cross section maximum in terms of the recovery of the cross section following the Cooper minimum seen in bands A and B. Another effect which could explain the feature is that of a p → d giant resonant enhancement, which causes significant modification to the cross sections of bands whose associated MOs possess appreciable d-orbital character. Although they are not metal d-orbital-localized, a d-orbital contribution to the MOs ionizing under band (C+D) should manifest itself in a cross section modification compatible with a Fano profile[71,72] in the region of the Ti 3p absorption edge; Ti 3p AOs ionize just below 40 eV ($^2P_{3/2}$ = 38 eV, $^2P_{1/2}$ = 39 eV[40]). The RPPICS of band C+D shows a minimum at 38 eV followed by a maximum around 49 eV. Calculation of the 3p−2e and 3p−4t_2 promotion energies for $TiCl_4$ gave values of 35.3 and 36.2 eV, respectively. The experimental spread of the $3p^53d^1$ configuration is 14.99 eV.[73] The e_2 band of Ti(η-C_7H_7)(η-C_5H_5) shows a strong feature with similar photon energy values for the minimium and maximum.[74] However, such an interpretation of this cross section feature is called into question by the cross section calculations discussed below.

The cross section behavior of band E is different from that of any of the other bands, with more features superimposed upon the general falloff. A sharp maximum at 20 eV is followed by another at 25 eV, and the cross section reaches a minimum at 38 eV before undergoing a broad gentle enhancement with a somewhat sharper maximum at 40 eV.

(iii) Cross Section Calculations. The calculated photoionization cross section for the valence levels with l_{out} = 10 are shown in Figure 5. It is noteworthy that the results obtained from the present study are in qualitative agreement with a previous MS−Xα calculation employing very different sphere parameters.[7] Strong shape resonances[75] are observed for all valence orbitals about 3 eV above the respective ionization thresholds. These shape resonances are due to excitations to quasi-bound Ti−Cl antibonding orbitals of t_2 symmetry. Unfortunately, due to instrumental limitations, these resonances cannot be identified from the experiment. The calculated photoionization cross sections decrease rapidly about 10 eV above the ionization threshold. However, there are interesting features at 40−50 eV photon energy (inset, Figure 5) that may help to characterize the nature of the orbitals. In this energy region, the higher binding energy $2a_1$ and $2t_2$ orbitals show a broad resonance. In contrast, the cross sections of other valence orbitals exhibit a minimum at 48 eV. The trends obtained from the calculations are in qualitative agreement with the RPPICSs determined from experiment.

A more stringent test of the accuracy of the calculation is to compare the branching ratio of the photoionization bands. The experimental and theoretical branching ratios are compared in Figure 6. Bands A and B are fairly distinct in the experimental spectra and can be unambiguously assigned to ionization from the $1t_1$ and $3t_2$ orbitals, respectively. The good agreement between the experimental and calculated branching ratios supports these assignments. It is noteworthy that both the magnitude and the position of the minimum in the cross section at 48 eV are reproduced correctly by the theory.

The assignment of bands (C+D) and E has been controversial. There are two possible assignments. The DV−Xa and previous Green's function[19] calculations suggest that band (C+D) be assigned to ionization from $2t_2$ and 1e orbitals and band E is due to the $2a_1$ ionization. On the other hand, MS−Xα calculation suggests that band (C+D) can be assigned to $2a_1$ and 1e orbitals and band E to $2t_2$. Both comparisons are made in Figure 6. The agreements between the experimental values for bands (C+D) and the calculated values for the ($2t_2$+1e) orbitals and the experimental values for band E and the calculated values for the $2a_1$ orbital are far superior to those

(71) Fano, U. *Phys. Rev.* **1961**, *124*, 1866.
(72) Fano, U.; Cooper, J. W. *Phys. Rev. A* **1965**, *137*, 1364.
(73) Sugar, J.; Corliss, C. *J. Phys. Chem. Ref. Data* **1985**, *14*, Suppl. 2.
(74) Green, J. C.; Kaltsoyannis, N.; Sze, K. H.; MacDonald, M. A. *J. Am. Chem. Soc.* **1994**, *116*, 1994.
(75) *Resonances in Electron and Molecular Scattering, van der Waals Complexes and Reactive Dynamics*; Truhlar, D. G., Ed.; American Chemical Society: Washington DC, 1984.

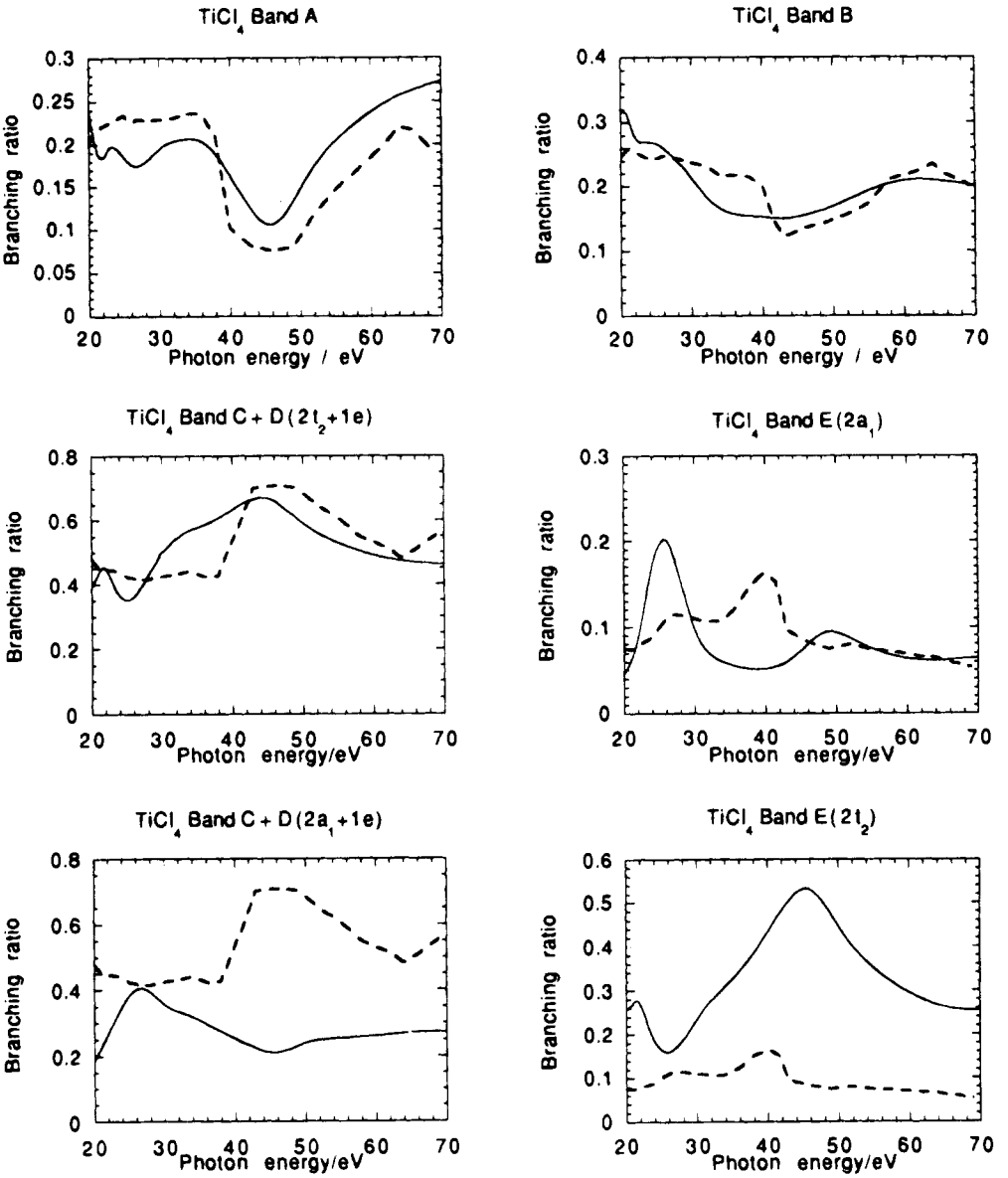

Figure 6. Comparison of theoretical (solid line) and experimental (dashed line) branching ratios for the photoelectron bands in $TiCl_4$. The two possible assignments (see text) of bands (C+D) and E are shown in the lower panels.

obtained for the MS−Xα assignment. For band (C+D), a maximum in the branching ratio was observed at 46 eV, which agrees with the calculated result if the band is composed of $2t_2$ and 1e ionizations. Two peaks were observed in the branching ratio of band E at 28 and 42 eV. These features can be correlated with the calculated peaks at 26 and 48 eV for the $2a_1$ ionization. The alternative assignments for bands (C+D) and E gave substantially inferior agreement with the experimental observations. For example, the calculated branching ratio profile for the $2a_1$ + 1e combination band is completely different from experiment.

It is interesting to speculate on the nature of the weak resonance in the $2t_2$ and $2a_1$ orbitals. It is likely the resonances are due to multiple scattering from the localized Cl electrons, since these orbitals are primarily Cl 3p in character. There exists an inverse relationship between the energy of the resonance above threshold (E) to the interatomic distance (R): E (eV) = $151/R^2$ (Å^3).[76,77] Using the $2a_1$ orbital, the maximum in the broad resonance is calculated to be at 49 eV and the ionization energy is 14 eV, then E is about 35 eV and the scattering distance is 2.1 Å . This distance is remarkably close to the Ti-Cl bond length of 2.185 Å which suggests that the resonance may be due to the scattering of the photoelectron originating from the Cl atom by the Ti atom.[78] The higher energy valence orbitals ($1t_1$, $3t_2$, and 1e) are mostly Cl 3p lone pairs, and the minimum in the photoionization cross section at about 40 eV may be associated with the Cooper minimum of the atomic Cl 3p orbital.[69,70]

Inspection of Figure 6 shows that at photon energies less than 42 eV the calculation overestimates the branching ratio of band (C+D) whereas at higher photon energies it underestimates it. The calculation is restricted to direct ionization and does not include possible p → d resonance followed by SCK decay in its estimate of a cross section. If such a process were indeed occurring in the anticipated photon energy region (*vide supra*), such a discrepancy would be expected in that such resonances generally have a Fano profile with a *minimum* in the cross

(76) Tse, S. *J. Chem. Phys.* **1988**, *89*, 920.
(77) Natoli, C. R. In *EXAFS and Near Edge Structure III*; Hodgson, K. O., Hedman, B., and Penner-Hahn, J. E., Eds.; Springer: New York, 1984.
(78) Addison-Jones, B. M.; Tan, K. H.; Yates, B. W.; Cutler, J. N.; Bancroft, G. M.; Tse, J. S. *J. Electron Spectrosc. Relat. Phenom.* **1989**, *48*, 155.

section followed by a *maximum*. As the branching ratios are all interdependent, the presence of such a resonance in the experimental cross section of band (C+D) would improve the agreement between theory and experiment for the other bands also.

Conclusion

The theoretical and experimental data presented here strongly favor the assignment

band	A	B	(C+D)	E
state	$^2T_1$	$^2T_2$	^2E, $^2T_2$	$^2A_1$

Good agreement between theory and experiment exists both with the IE predicted by the DV−Xα calculations and with the branching ratios found by MS−Xα calculation. Shape resonances are found in the $2t_2$ and $2a_1$ orbital cross sections due to multiple scattering from the localized Cl electrons. The minimum in the $3t_2$ cross section is associated with the Cooper minimum in the Cl 3p orbital. Though a maximum in the cross section between 40 and 50 eV is predicted for $2t_2$ on the basis of one-electron calculations, that observed may well be enhanced by a Ti 3p → 3d resonant process.

Acknowledgment. We wish to thank the machine staff of Daresbury Laboratory for their efficient running of the Synchrotron Radiation Source and the Science and Engineering Research Council for financial support. N.K. thanks the Graduate School of The Ohio State University and the SERC/NATO for Postdoctoral Fellowships. B.E.B. gratefully acknowledges the support of the Division of Chemical Sciences, Office of Basic Energy Sciences, U.S. Department of Energy (Grant DE-FG02-86ER13529).